

Supporting Information

A pyrimidine end-capped electron transport material interacted with silver improving electron-injection and long-term stability in OLED

Yuhui Chen ^[a], *Takeshi Sano* ^{*[b]}, *Hisahiro Sasabe* ^{*[a], [c], [d]}, *Ryo Sugiyama* ^[a], *Amane Matsunaga* ^[a], *Hiroki Sato* ^[a], *Hiroshi Katagiri* ^{[a], [c], [d]}, and *Junji Kido* ^{*[a], [b], [c], [d]}

Department of Organic Materials Science, Yamagata University, 4-3-16 Jonan, Yonezawa, Yamagata 992-8510, Japan.

E-mail: takeshi.sano@yz.yamagata-u.ac.jp, h-sasabe@yz.yamagata-u.ac.jp, kid@yz.yamagata-u.ac.jp

Table of Contents

1. General Information and Methods	S2
2. Theoretical calculations.....	S3
3. Synthesis.....	S5
4. Thermal property.....	S11
5. Photophysical property.....	S12
6. Fabrication and characterization of OLEDs.....	S17
7. References.....	S23

1. General Information and methods

1.1 Theoretical calculation, synthesis and characterization of the materials:

Quantum chemical calculations were performed using the hybrid density functional theory (DFT) functional Becke and Hartree-Fock exchange and Lee Yang and Parr correlation (B3LYP) as implemented by the Gaussian 09 program packages. The molecular structure optimizations were performed at the B3LYP/6-31G(d) level. The E_S and E_T values were obtained from time-dependent (TD)-DFT calculation at the B3LYP/6-31G(d) level. ^1H NMR spectra were recorded on JEOL 600 (600 MHz) spectrometer. Mass spectra were obtained using a Waters SQD2 mass spectrometer with atmospheric pressure solid analysis probe (ASAP). TGA was undertaken using a SEIKO EXSTAR 6000 TG/DTA 6200 unit under nitrogen atmosphere at a heating rate of $10\text{ }^\circ\text{C min}^{-1}$. DSC was performed using a Perkin-Elmer Diamond DSC Pyris instrument under nitrogen atmosphere at a heating rate of $10\text{ }^\circ\text{C min}^{-1}$. UV-vis spectra were measured using a Shimadzu UV-2600 UV-vis spectrophotometer. Photoluminescence spectra were measured using a FluoroMax-2 (Jobin-Yvon-Spex) luminescence spectrometer. The I_p was determined by the PYS^[1] using a Sumitomo Heavy Industries, Ltd PYS-201 under the vacuum ($\sim 10^{-3}$ Pa). XRD data for **TPy-BP** and **DPmPy-BP** were collected on a Rigaku Saturn 724 charged-coupled-device (CCD) diffractometer using $\text{MoK}\alpha$ ($\lambda = 0.71073\text{ \AA}$). Single crystals of **TPy-BP** and **DPmPy-BP** suitable for X-ray analysis were grown by slow gradient sublimation. Data collection, cell refinements, and data reductions were conducted using the CrysAlisPro^[2] software. The structure was solved by direct methods using the SHELXT program and were refined by full-matrix least-squares methods on F2 using SHELXL2014^[3]. All materials for publication were prepared using the Yadokari-XG 2009 software^[4]. The UPS and XPS data were measured using X-ray photoelectron spectrometer (ThermoFischer, Thermo Fisher Scientific Theta probe) under the operational vacuum pressure of 3×10^{-6} Pa. The total time of exposure to air was under 5 mins for all samples. For the UPS, energy of power source was 21.22 eV (HeI excitation source). A bias of -8.0 V was applied to separate the sample and the secondary edge for the analyzer while the accumulated signal was obtained in 5 cycles.

1.2 Fabrication of OLEDs and characterization:

The substrates were cleaned with ultra-purified water and organic solvents, and then dry-cleaned for 10 minutes by exposure to UV-ozone. All organic materials, Ag and Al were thermally evaporated under vacuum ($\sim 10^{-5}$ Pa). Shadow masks were used to define the pixel size of 0.04 cm^2 . The thickness and deposition rate were monitored in situ during deposition by an oscillating quartz thickness monitor. The electroluminescent (EL) were taken using an optical multichannel analyzer Hamamatsu Photonics PMA-11. The current density-voltage and luminance-voltage characteristics were measured by using a Keithley source measure unit 2400 and a Minolta CS200 luminance meter, respectively. The operational lifetime of the OLED devices was measured by an EHC ELS-100 OLED aging testing system.

2. Theoretical calculations

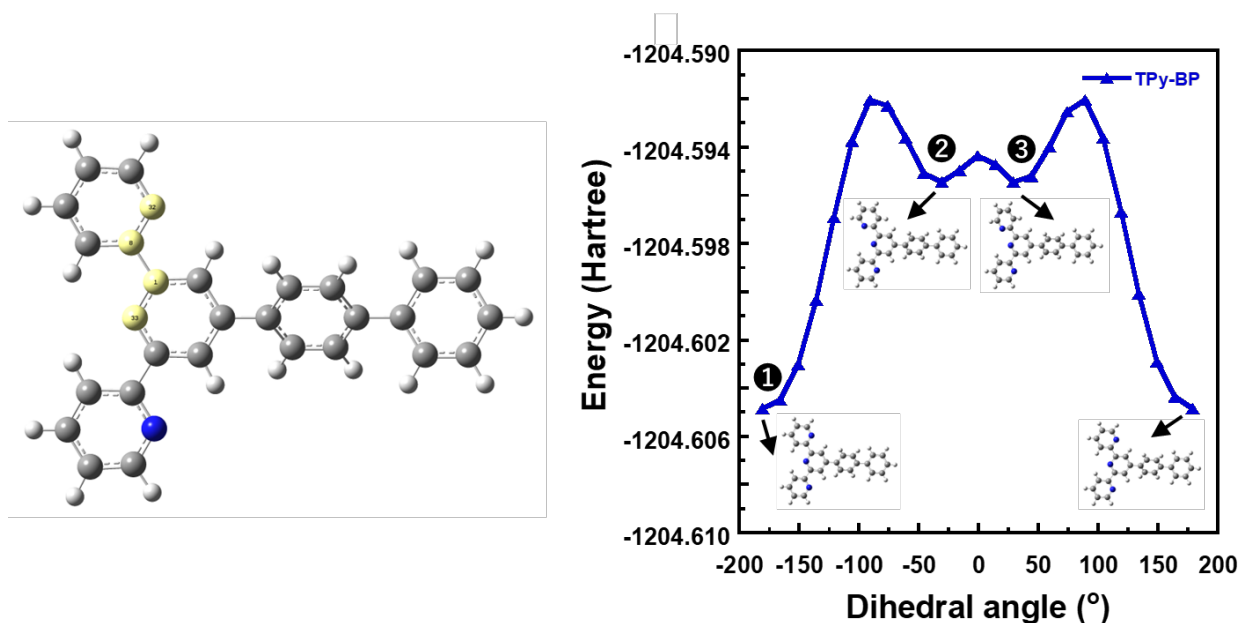


Figure S1. The PES scan of TPY-BP performed at the B3LYP/ 6-31G(d) level by changing the N32-C8-C1-N33 (marked as yellow color) torsion angle in 15° steps from -180.87° to +179.13° (inset: the most stable conformation isomer).

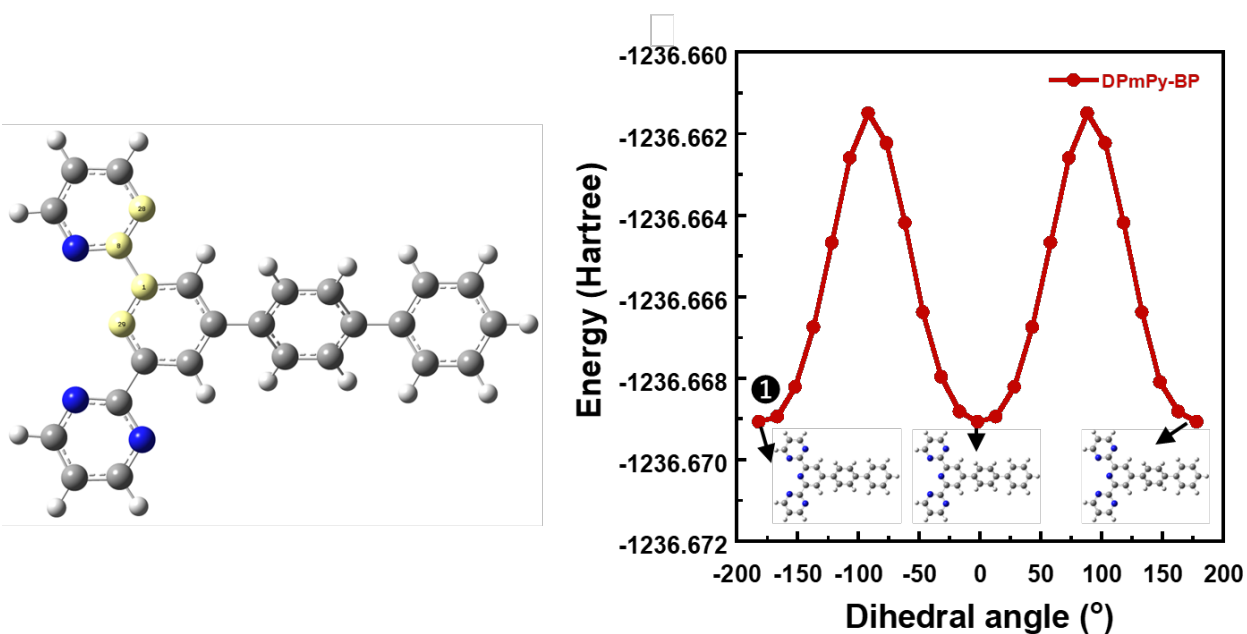


Figure S2. The PES scan of DPmPy-BP performed at the B3LYP/ 6-31G(d) level by changing the N28-C8-C1-N29 (marked as yellow color) torsion angle in 15° steps from -181.85° to +178.15° (inset: the most stable conformation isomer).

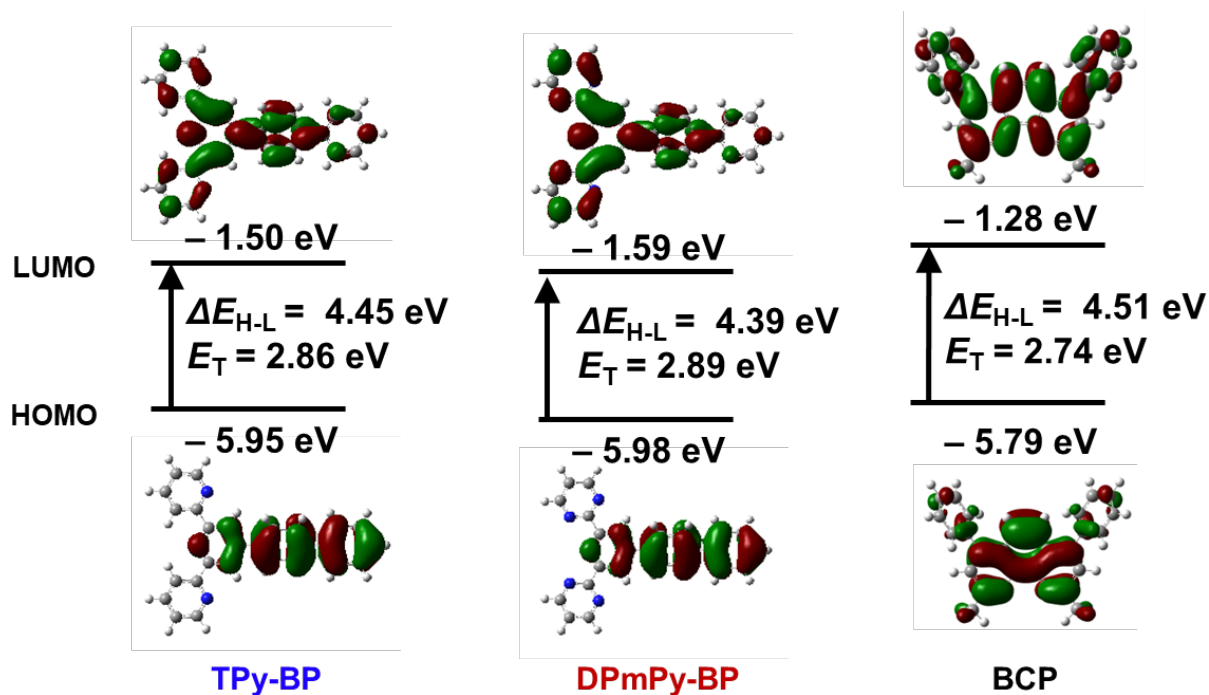


Figure S3. Chemical structures, HOMO/LUMO distribution of TPy-BP, DPmPy-BP and BCP.

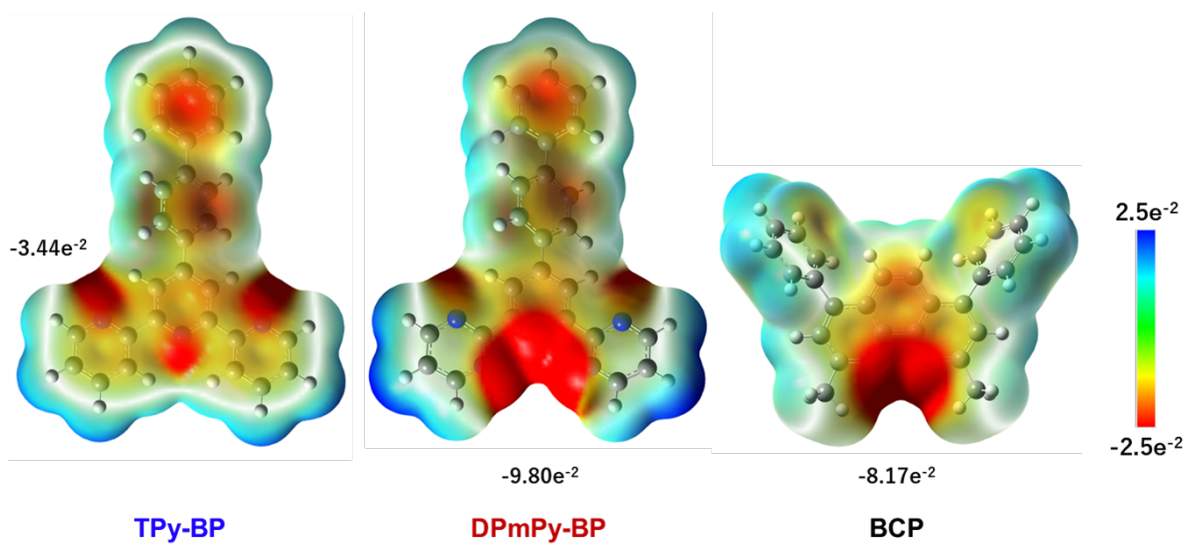


Figure S4. The ESP maps of TPy-BP, DPmPy-BP and BCP.

3. Synthesis

BCP was purchased from Sigma Aldrich. **TPy-BP** was prepared according to the literature. ^[5]

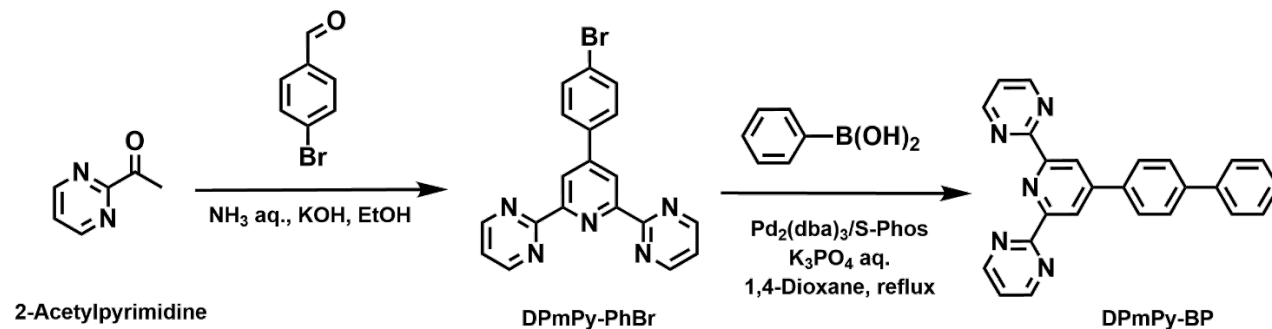


Figure S5. Synthetic route of **DPmPy-BP**.

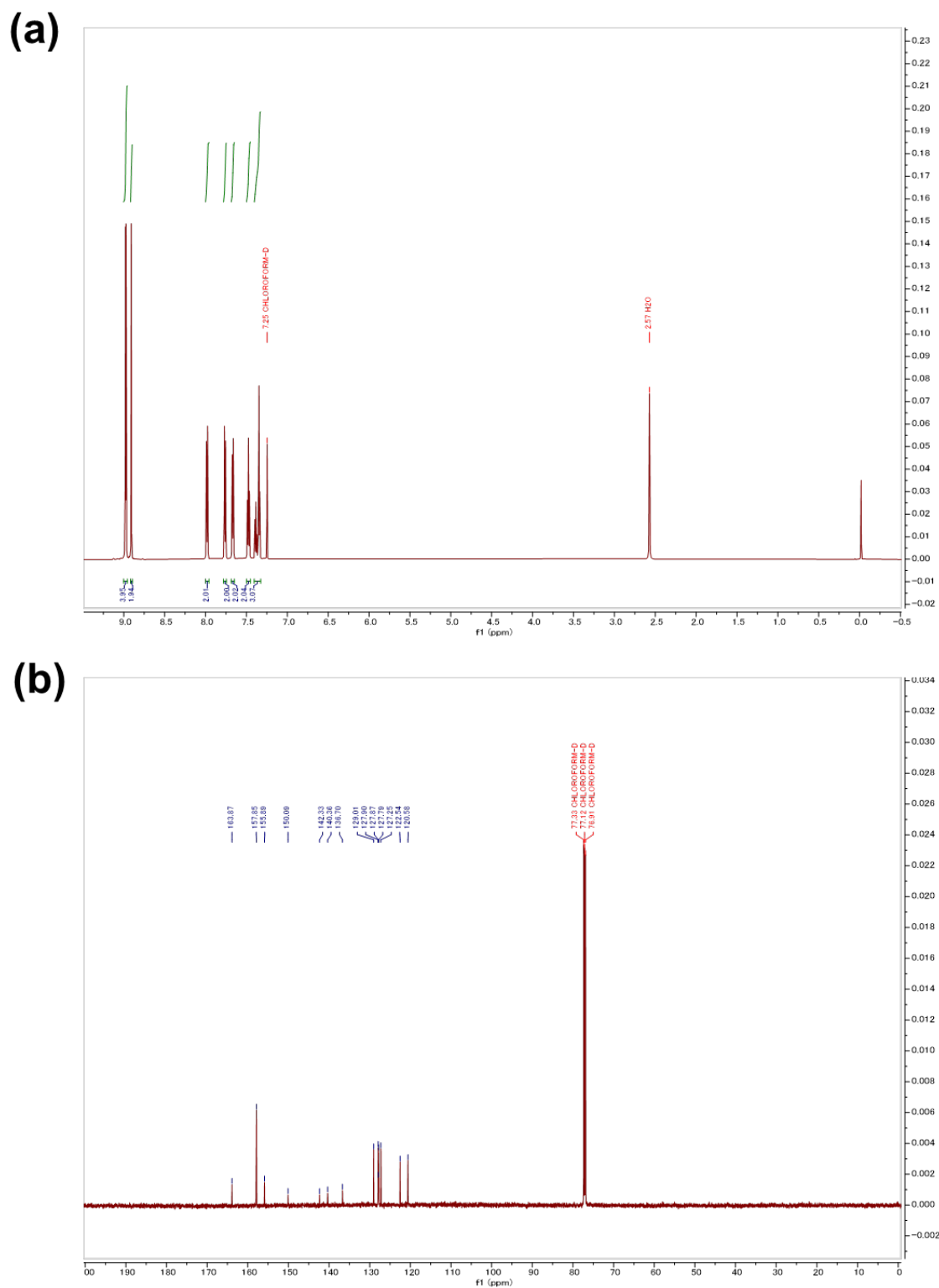
Synthesis of **DPmPy-PhBr**:

A mixture of 4-bromobenzaldehyde (2.01 g, 11.6 mmol), 2-acetylpyrimidine (2.89 g, 23.7 mmol), KOH (1.24 g, 21.9 mmol), EtOH (100 mL), and 28% aqueous NH₃ (100 mL) were stirred for 30 h at 50 °C. The precipitate was filtered, washed with ethanol next to water, and recrystallized through toluene to offer **DPmPy-PhBr** (2.80 g, 62.1%) as a grey white solid; ¹H-NMR (400 MHz, CDCl₃) δ 9.04 (s, 2H), 8.76 (d, J = 4.4 Hz, 2H), 8.67 (d, J = 8.0 Hz, 2H), 8.04 (d, J = 8.0 Hz, 1H), 7.92-7.87 (m, 2H), 7.70 (t, J = 8.0 Hz, 1H), 7.55 (d, J = 8.4 Hz, 1H), 7.39-7.36 (m, 2H) ppm; MS (ASAP): m/z 391 [M+H]⁺.

Synthesis of **DPmPy-BP**:

DPmPy-PhBr (2.74 g, 7.05 mmol), phenyl boronic acid (1.30g, 10.6 mmol), 1,4-dioxane (120.0 mL), and tripotassium phosphate (12.49 g, 58.8 mmol) in 45 mL H₂O were added to a 300 mL round bottom flask. After 1 h of nitrogen bubbling through the mixture, 4 mol% S-Phos 0.156 g, 2 mol% Pd₂(dba)₃ 0.170 g was added, and the mixture was stirred for 48 hours at reflux temperature under N₂ flow. The precipitate was filtered, washed by water and methanol. Then the purification underwent through recrystallization from toluene, and further purified by train sublimation to yield **DPmPy-BP** (1.58 g, 58.1%) as a white solid: ¹H-NMR (400 MHz, CDCl₃) δ 9.00 – 8.95 (m, 4H), 8.91 (d, J = 1.0 Hz, 2H), 7.98 (d, J = 8.1 Hz, 2H), 7.76 (d, J = 8.0 Hz, 2H),

7.69 – 7.64 (m, 2H), 7.48 (t, J = 7.5 Hz, 2H), 7.41 – 7.32 (m, 3H) ppm; ASAP MS: m/z 389 [M+H]⁺.
¹³C-NMR (150 MHz, CDCl₃) δ 163.87, 157.85, 155.89, 150.09, 142.33, 140.36, 136.70, 129.01, 127.90, 127.87, 127.79, 127.25, 122.54, 120.58; Anal calcd for C₂₅H₁₇N₅: C, 77.50; H, 4.42; N, 18.08%. Found C, 77.71; H, 4.36; N, 18.01%.



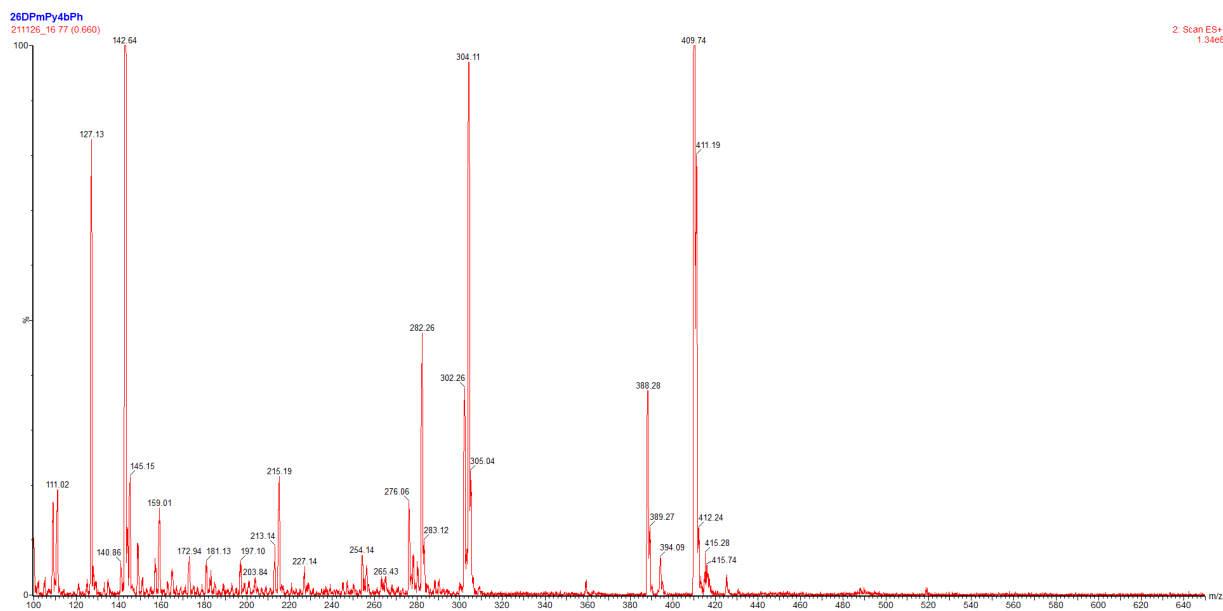


Figure S7. Mass spectrum of DPmPy-BP.

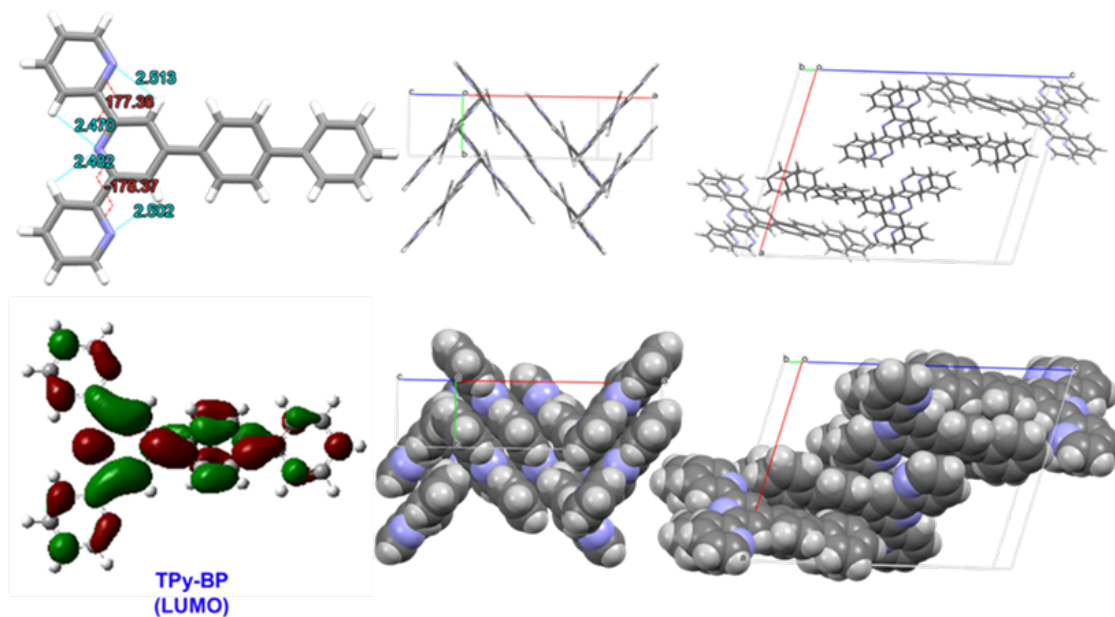


Figure S8. The crystal structures, packing mode and partial view of **TPy-BP**, for which the existing LUMO are illustrated as space-filling models.

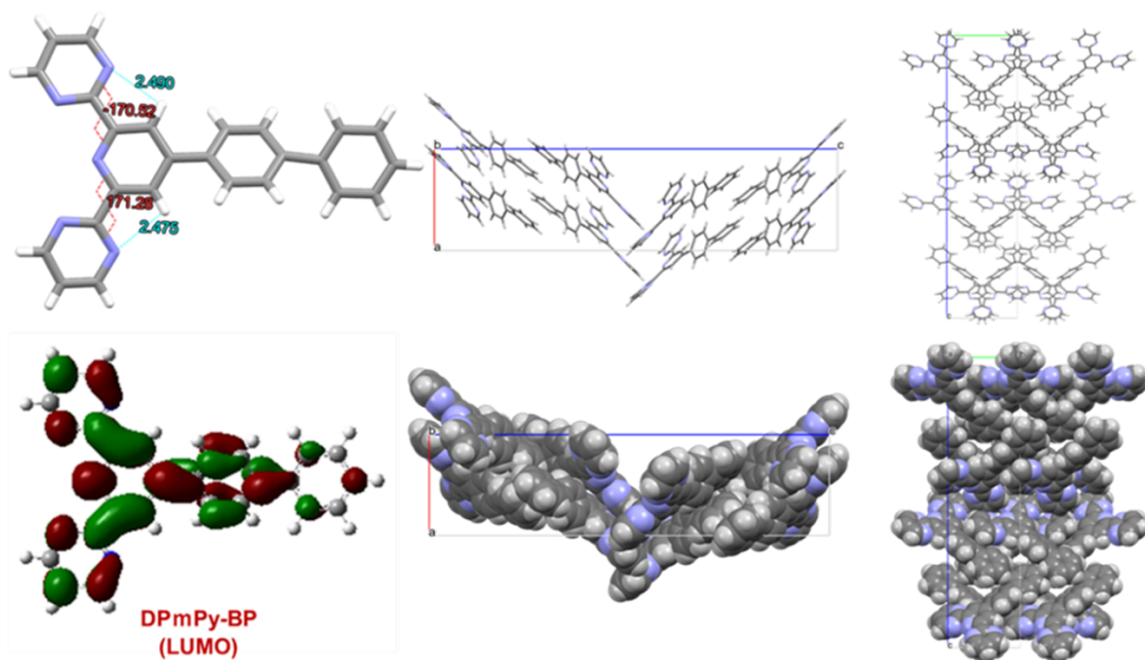


Figure S9. The crystal structures, packing mode and partial view of **DPmPy-BP**, for which the existing LUMO are illustrated as space-filling models.

Table S1. Crystal data and structure refinement for **TPy-BP** and **DPmPy-BP**.

Compound	TPy-BP	DPmPy-BP
Empirical formula	C ₂₇ H ₁₉ N ₃	C ₂₅ H ₁₇ N ₅
Formula weight	385.45	387.43
Temperature (K)	150	150
Wavelength (Å)	0.71073	0.71073
Crystal system	Monoclinic	Orthorhombic
Space group	<i>P</i> 2 ₁ / <i>n</i>	<i>Pca</i> 2 ₁
<i>a</i> (Å)	16.6536(3)	9.9988(2)
<i>b</i> (Å)	5.4082(1)	9.8965(2)
<i>c</i> (Å)	22.4141(4)	39.6425(9)
α (°)	90	90
β (°)	106.231(2)	90
γ (°)	90	90
Volume (Å ³)	1938.29(6)	3922.75(14)
<i>Z</i>	4	8
Density (g/cm ³)	1.321	1.312
Absorption coefficient (mm ⁻¹)	0.079	0.081
F(000)	808.0	1616.0
Crystal size (mm ³)	0.100 × 0.040 × 0.010	0.100 × 0.040 × 0.010
Theta range for data collection (°)		
Index ranges	-20 ≤ <i>h</i> ≤ 20, -6 ≤ <i>k</i> ≤ 6, -28 ≤ <i>l</i> ≤ 28	-12 ≤ <i>h</i> ≤ 12, -12 ≤ <i>k</i> ≤ 12, -51 ≤ <i>l</i> ≤ 51
Reflections collected		
Independent reflections	4001 [R(int) =]	8959 [R(int) =]
Completeness (%)	100 ($\theta = 26.499^\circ$)	100 ($\theta = 27.496^\circ$)
Absorption correction	Semi-empirical from equivalents	Semi-empirical from equivalents
Max. and min. transmission	1.000 and 0.954	1.000 and 0.761
Refinement method	Full-matrix least-squares on F ²	Full-matrix least-squares on F ²
Data / restraints / parameters	4001 / / 344	8959 / / 578
Goodness-of-fit on F ²	1.097	1.050
Final R indices [I > 2σ(I)]	R1 = 0.0451, wR2 = 0.1178	R1 = 0.0428, wR2 = 0.1098
R indices (all data)	R1 = 0.0451, wR2 = 0.1178	R1 = 0.0428, wR2 = 0.1098
Largest diff. peak and hole (e·Å ⁻³)		

4. Thermal property

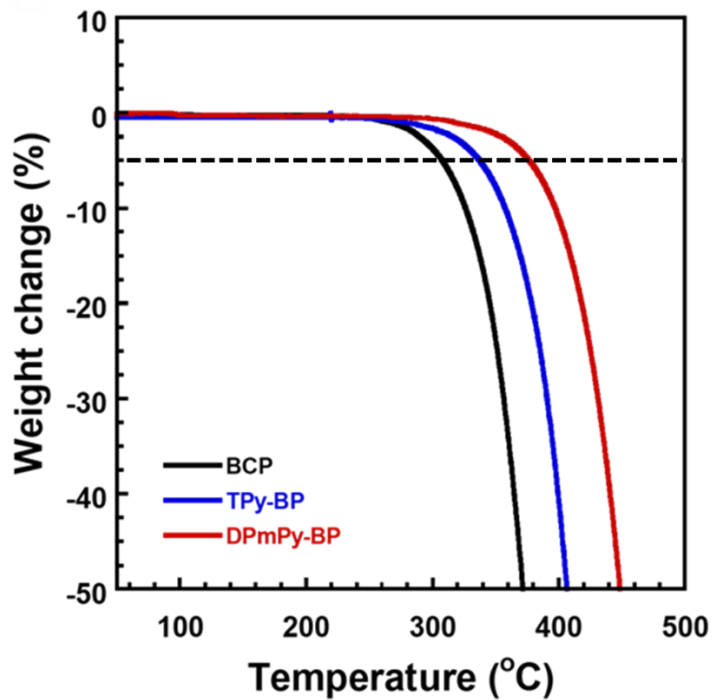


Figure S10. TGA curves for TPy-BP, DPmPy-BP and BCP. The heating rate was 10 °C/min under an N₂ atmosphere.

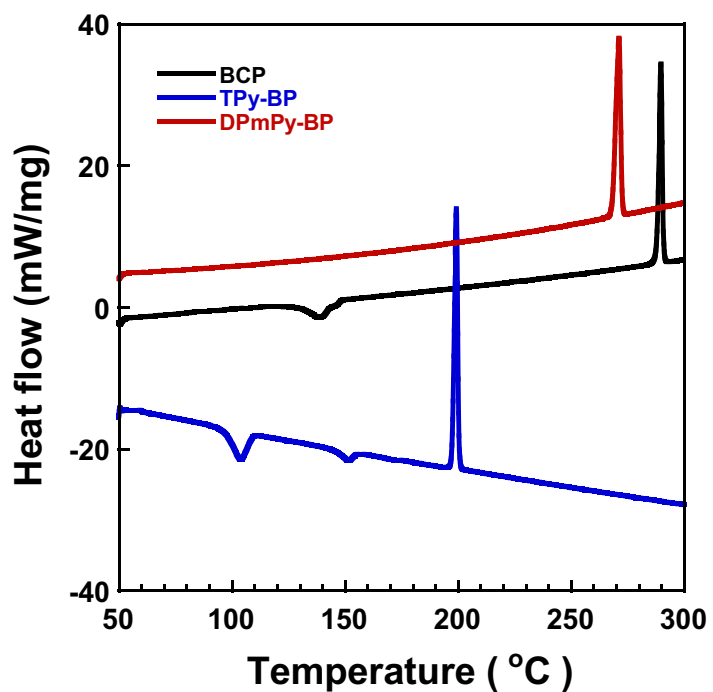


Figure S11. DSC curves for TPy-BP, DPmPy-BP and BCP. The heating rate was 10 °C/min under an N₂ atmosphere.

5. Physical property

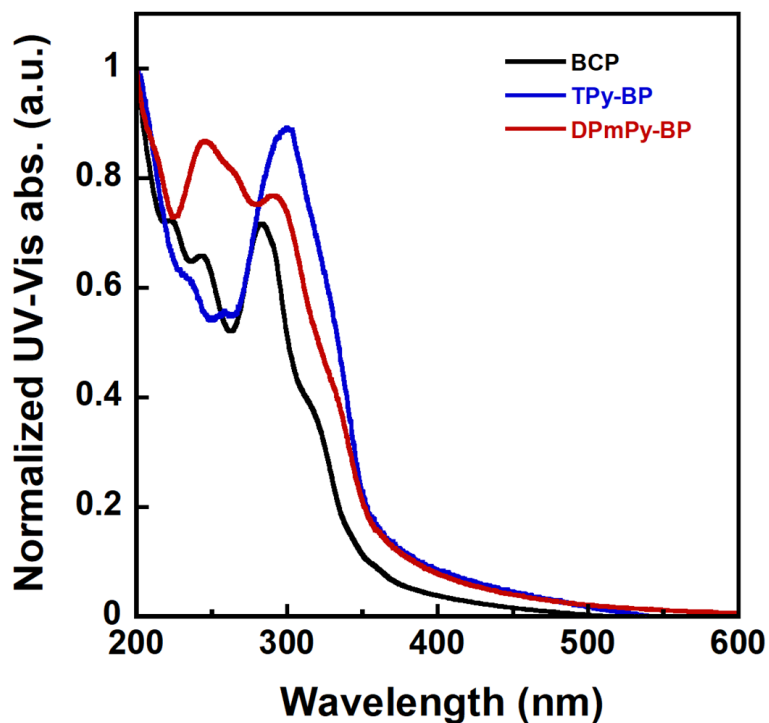


Figure S12. UV-vis spectra for TPy-BP, DPmPy-BP and BCP film.

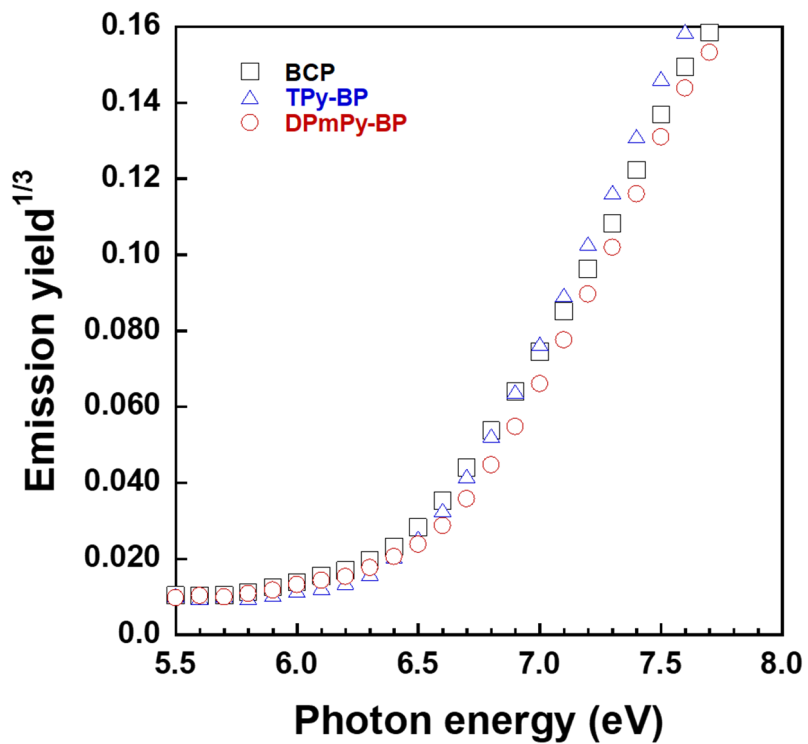


Figure S13. PYS spectra for TPy-BP, DPmPy-BP and BCP film.

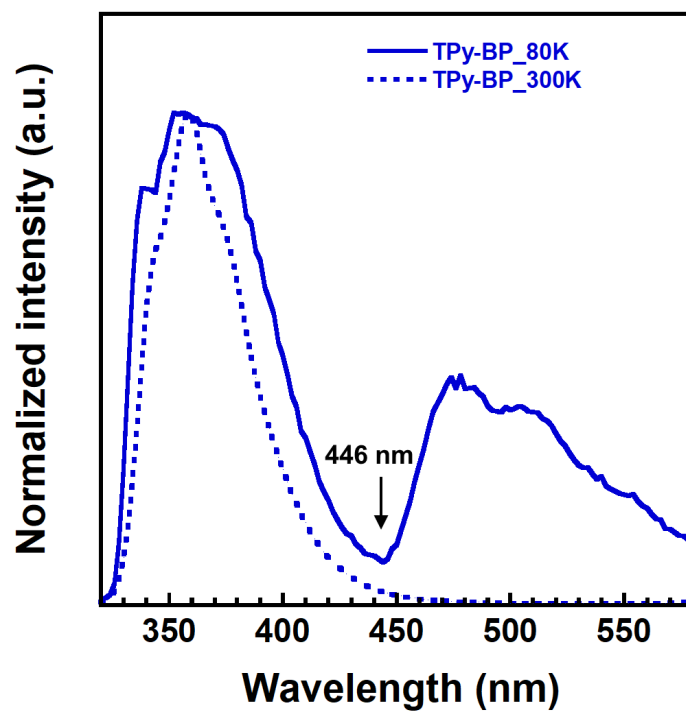


Figure S14. PL spectra for TPy-BP in 2-methyltetrahydrofuran (10^{-5} M) at 300 K and 80 K.

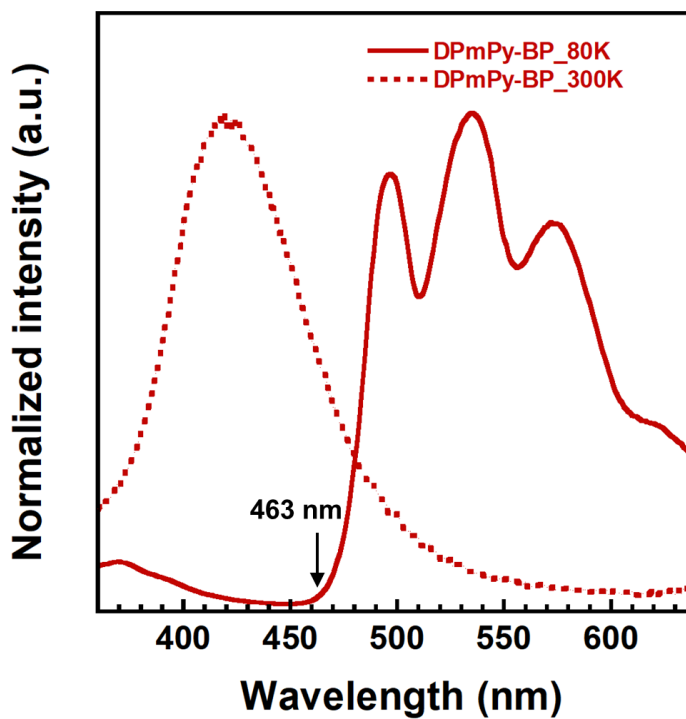


Figure S15. PL spectra for DPmPy-BP in 2-methyltetrahydrofuran (10^{-5} M) at 300 K and 80 K.

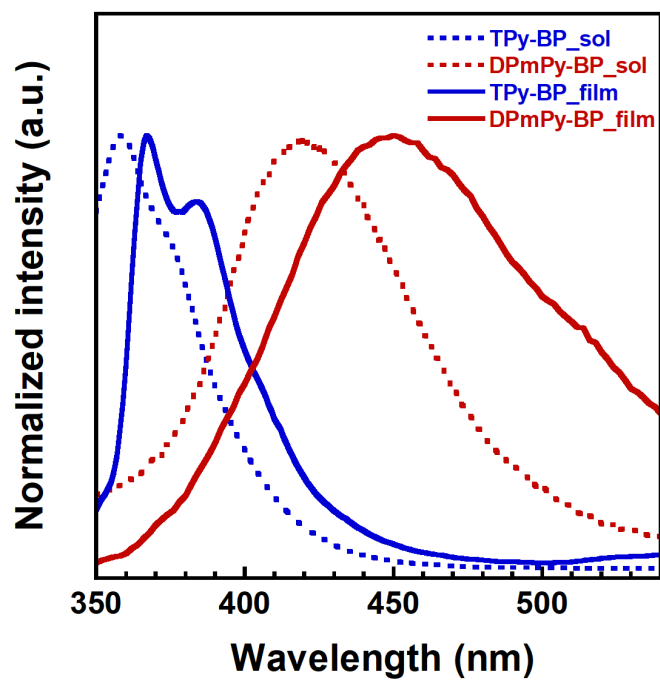


Figure S16. PL spectra for the neat films of TPy-BP and DPmPy-BP at 300 K.

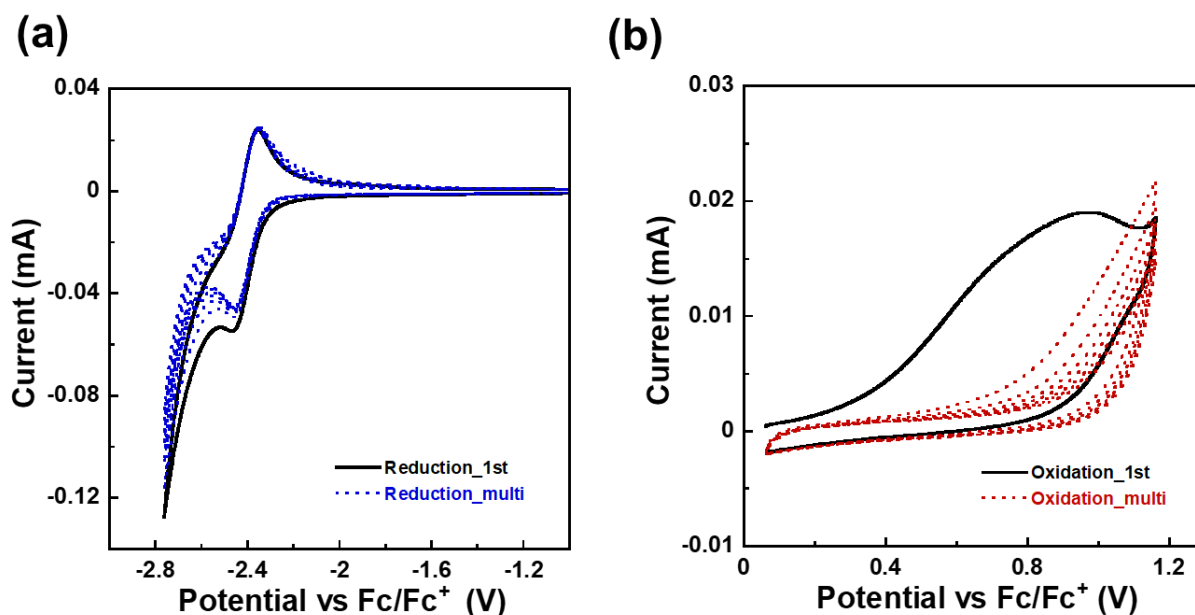


Figure S17. Cyclic voltammograms (CV) for TPy-BP vs ferrocene-ferrocenium Fc/Fc⁺ at room temperature. (a) Reduction CV in *N,N*-dimethylformamide (DMF). (b) Oxidation CV in dichloromethane (DCM).

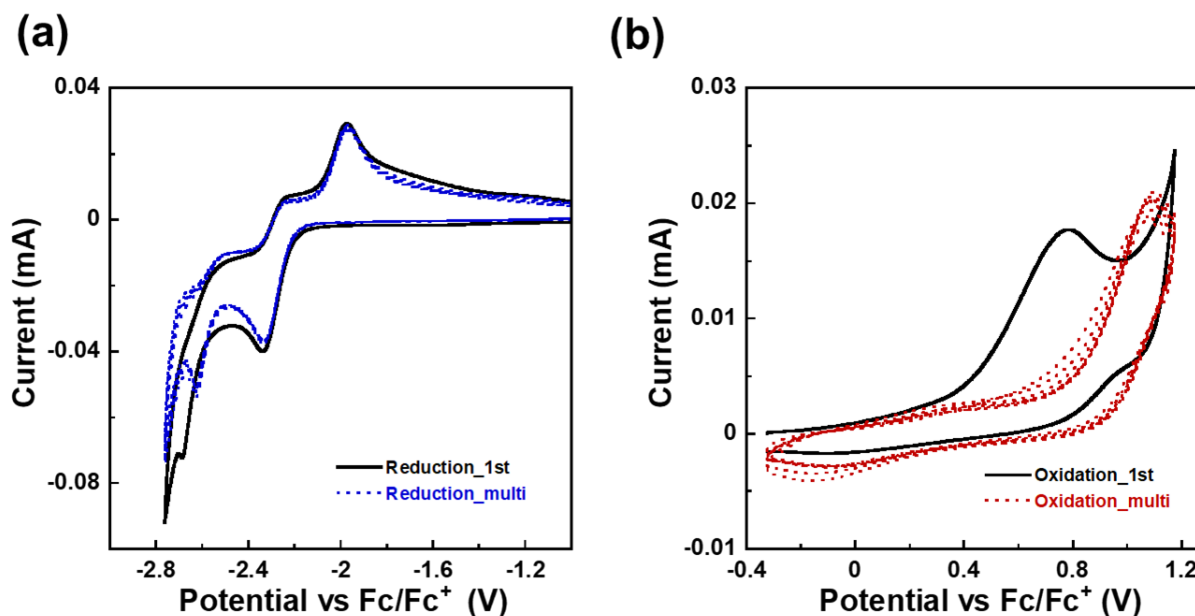


Figure S18. Cyclic voltammograms (CV) for DPmPy-BP vs ferrocene-ferrocenium Fc/Fc⁺ at room temperature. (a) Reduction CV in DMF. (b) Oxidation CV in DCM.

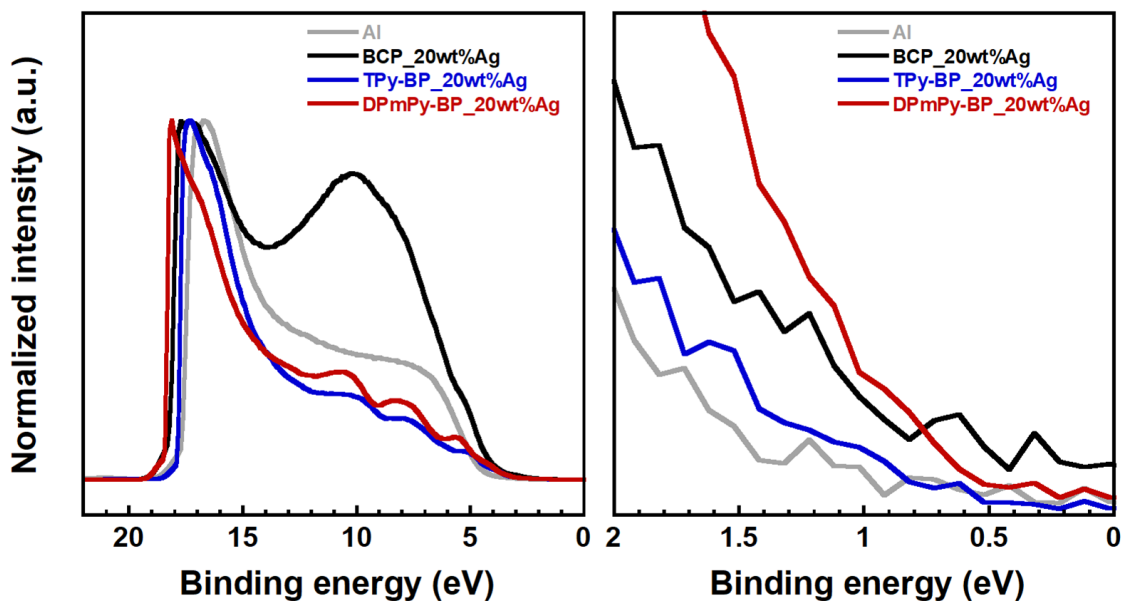


Figure S19. UPS spectra for Ag-doped TPy-BP, DPmPy-BP and BCP film.

Table S2. Details for the deposition of Ag-doping films.

ETMs	MW	Weight ratio (ETM:Ag)	Molar ratio ^a (ETM:Ag)	Volume ratio ^b (ETM:Ag)
BCP	360.5	80:20	1.20:1	4.88:0.116
TPy-BP	385.5	80:20	1.12:1	4.88:0.116
DPmPy-BP	387.4	80:20	1.11:1	4.88:0.116

a) The molar mass of Ag was set to 107.9. b) The density of Ag was set to 10.50 g cm⁻³ while those of ETMs were set to a unified value of 1.0 g cm⁻³.

6. Fabrication and characterization of OLEDs

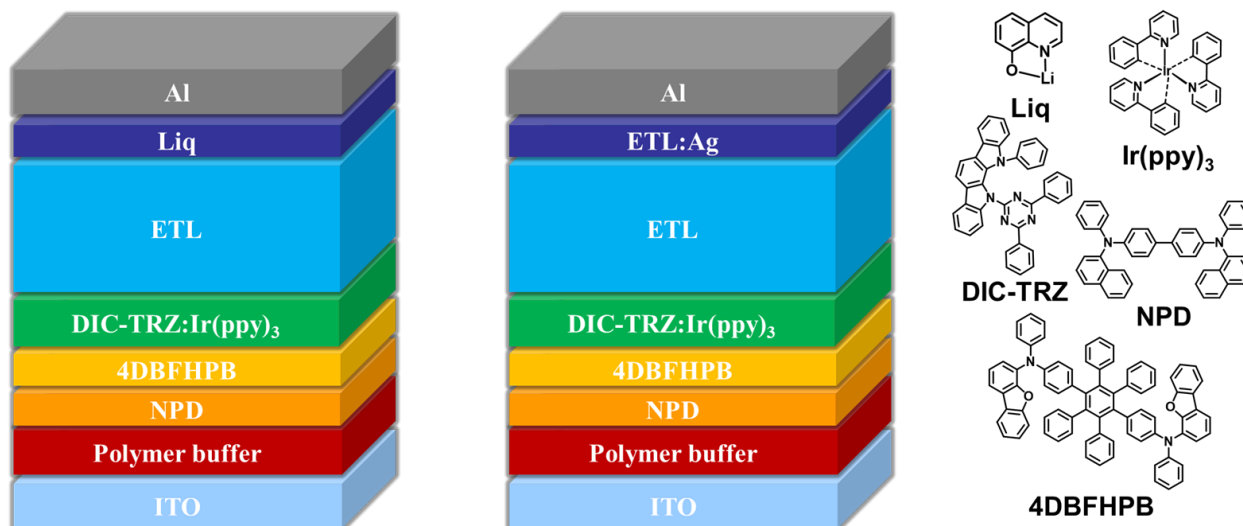


Figure S20. Device structures and chemical structures of materials used.

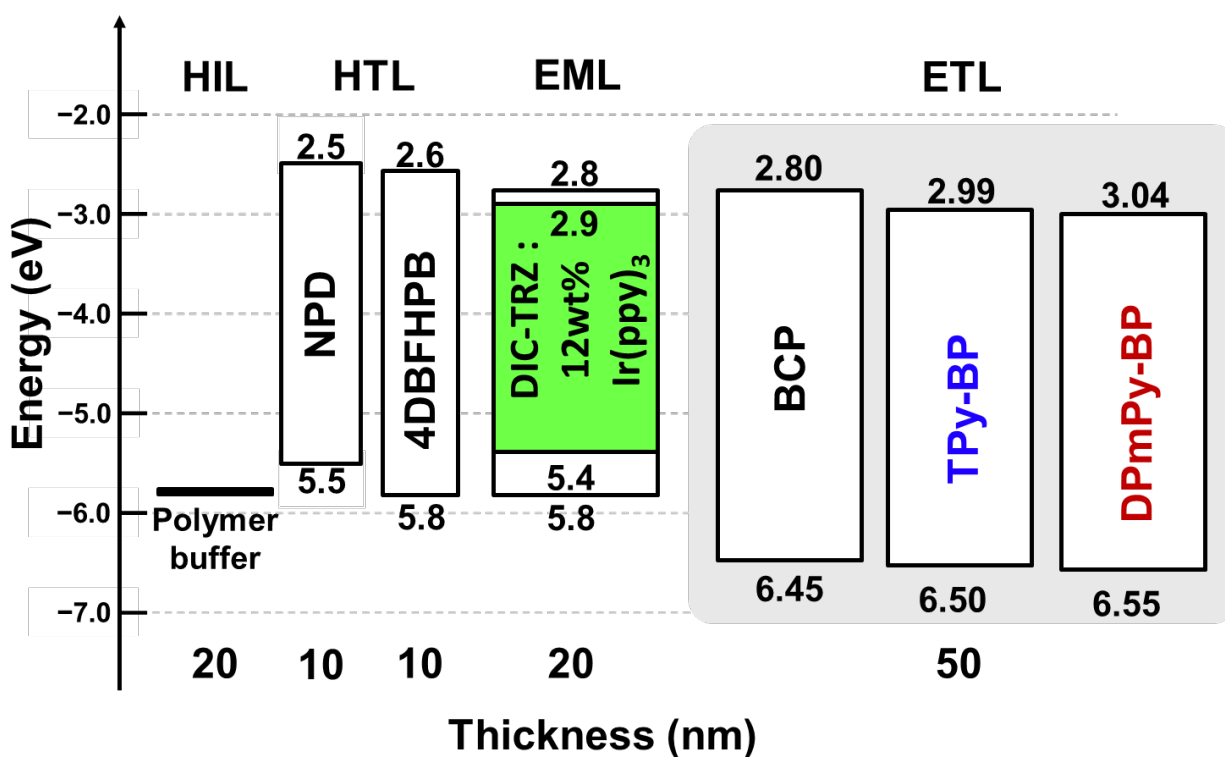


Figure S21. The energy diagram of OLED devices.

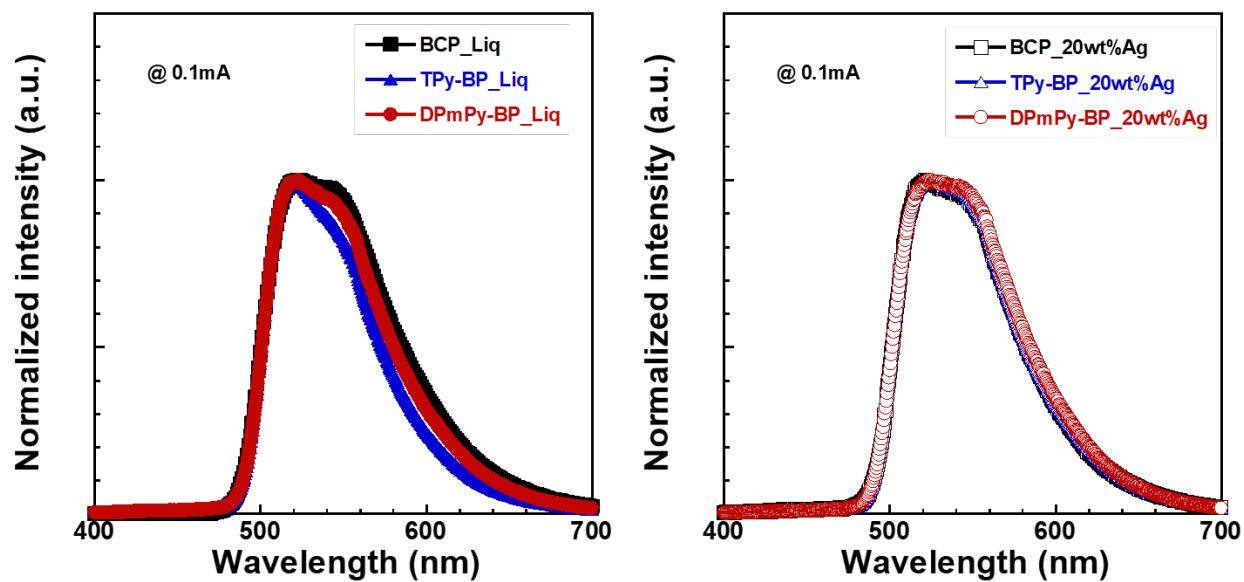


Figure S22. Normalized EL spectra.

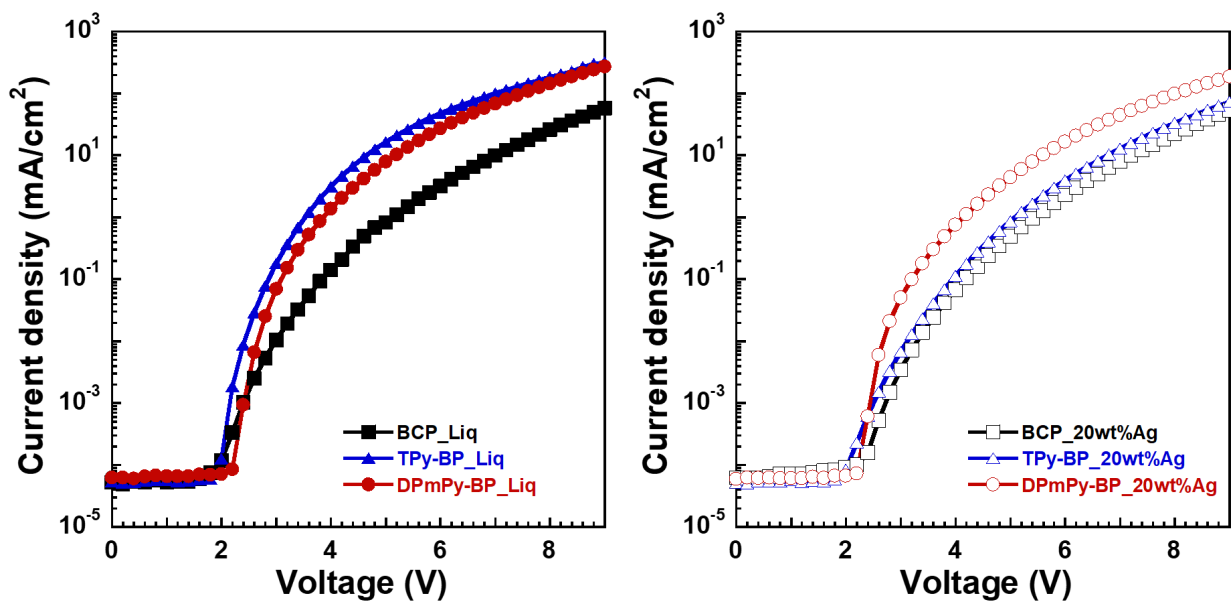


Figure S23. The current density versus voltage characteristics.

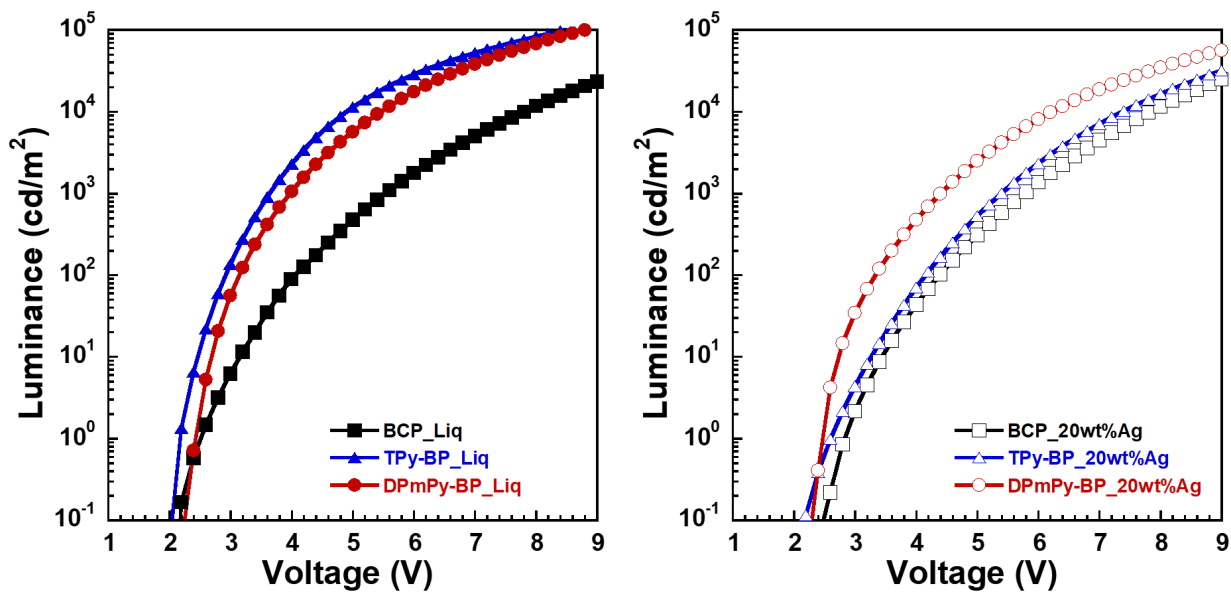


Figure S24. The luminance versus voltage characteristics.

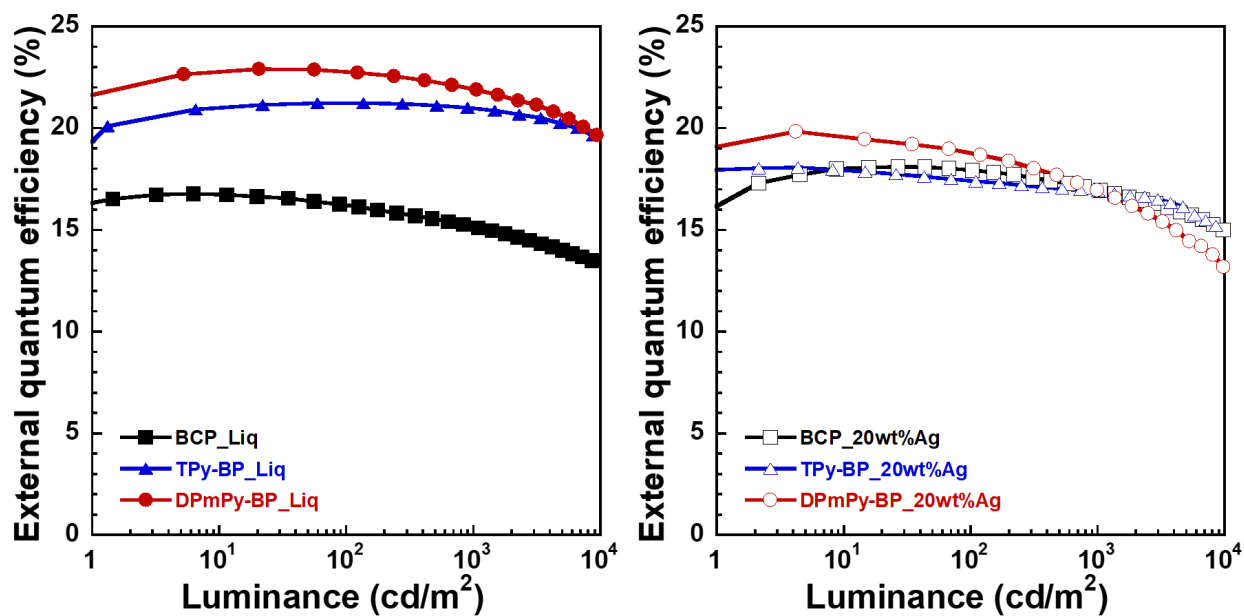


Figure S25. EQE versus luminance characteristics.

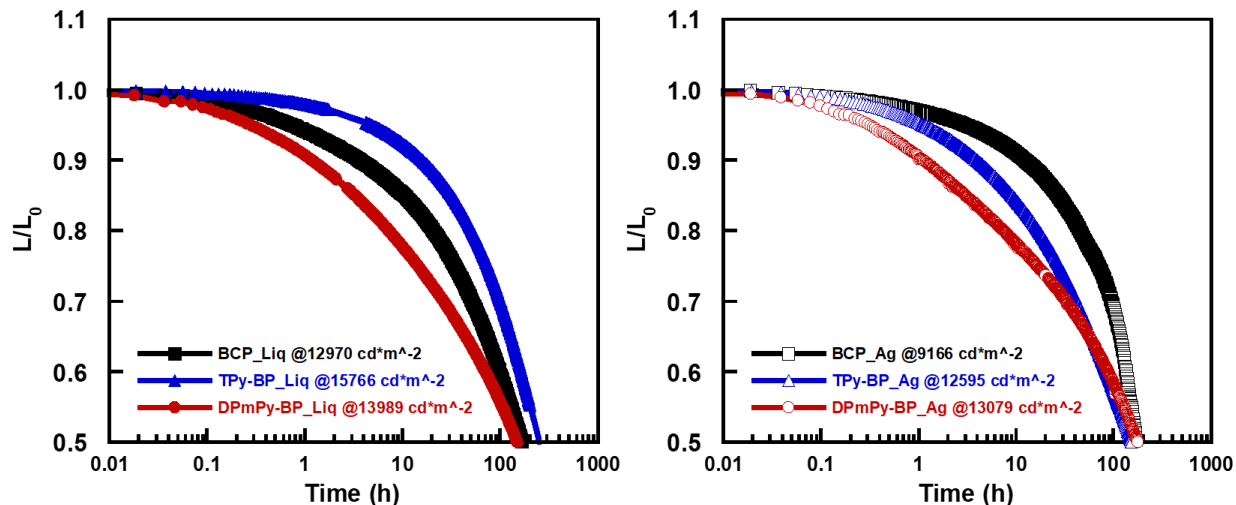


Figure S26. Operation lifetime of encapsulated devices till 50% of initial luminance at 25 mA cm⁻².

Table S3. Summary of OLED performance

electron-injection	ETM	V_{on} ^a [V]	$V_{100}/\eta_{p,100}/\eta_{c,100}/\eta_{ext,100}$ ^b [V/lm W ⁻¹ /cd A ⁻¹ /%]	$V_{1000}/\eta_{p,1000}/\eta_{c,1000}/\eta_{ext,1000}$ ^c [V/lm W ⁻¹ /cd A ⁻¹ /%]	LT ₅₀ ^d [h]
	BCP	2.49	4.10/ 45.1/ 59.2/ 16.2	5.52/ 31.7/ 55.7/ 15.7	14892
Liq	TPy-BP	2.15	2.91/ 82.5/ 76.2/ 21.2	3.63/ 65.1/ 75.3/ 21.0	32682
	DPmPy-BP	2.41	3.13/ 81.4/ 81.0/ 22.8	3.97/ 61.8/ 78.0/ 21.9	16291
	BCP	2.82	4.38/ 45.9/ 64.0/ 17.9	5.76/ 33.0/ 60.6/ 17.0	8305
ETM:Ag	TPy-BP	2.60	4.15/ 47.1/ 62.2/ 17.4	5.39/ 35.1/ 60.2/ 16.9	13641
	DPmPy-BP	2.43	3.32/ 63.7/ 67.3/ 18.8	4.40/ 43.3/ 60.6/ 16.9	16913

a) Turn on voltage (V_{on}) at 1 cd m⁻². b) Voltage (V), power efficiency (η_p), current efficiency (η_c) and external quantum efficiency (η_{ext}) at 100 cd m⁻². c) V , η_p , η_c and η_{ext} at 1000 cd m⁻². d) Operation lifetime at 50% (LT₅₀) at 1000 cd m⁻².

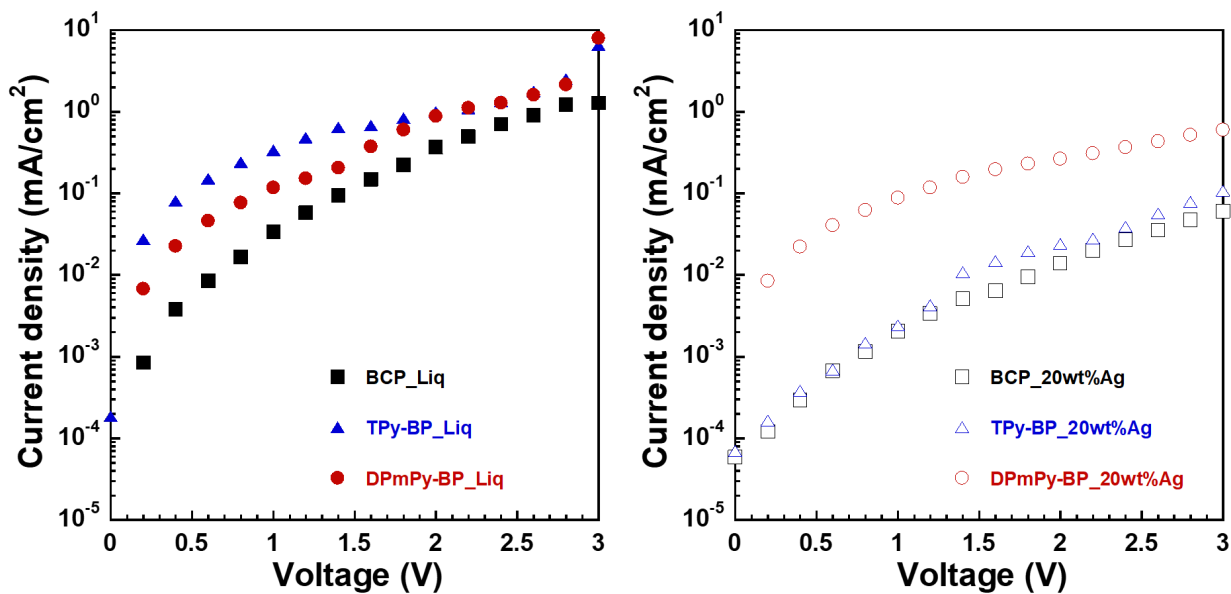


Figure S27. The current density versus voltage characteristics of EODs with structures of ITO/ETL (60 nm)/Liq (1 nm)/Al (100 nm) or ITO/ETL (55 nm)/ETL:Ag (5 nm, 20 wt%)/Al (100 nm).

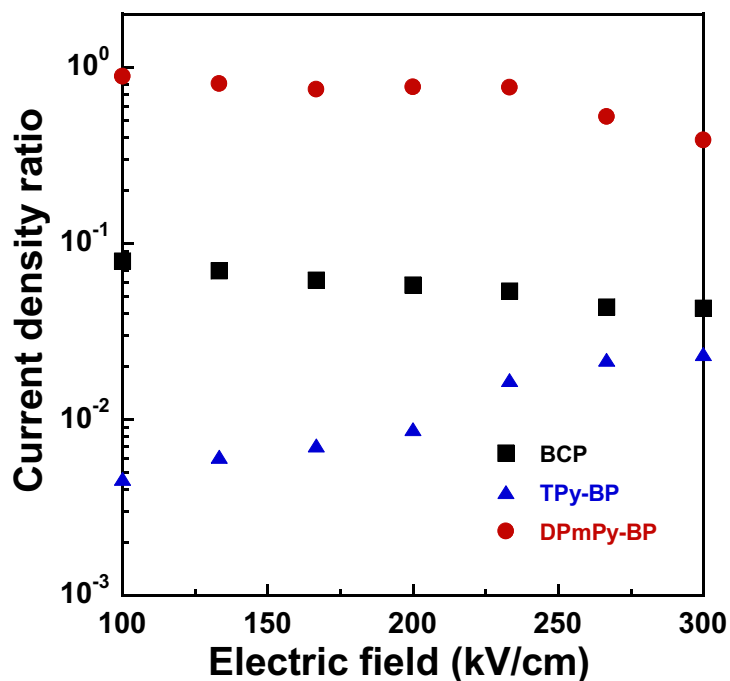


Figure S28. The current density ratio of Ag-doped ETMs to **Liq** based on EODs with structures of ITO/ETL (60 nm)/Liq (1 nm)/Al (100 nm) or ITO/ETL (55 nm)/ETL:Ag (5 nm, 20 wt%)/Al (100 nm).

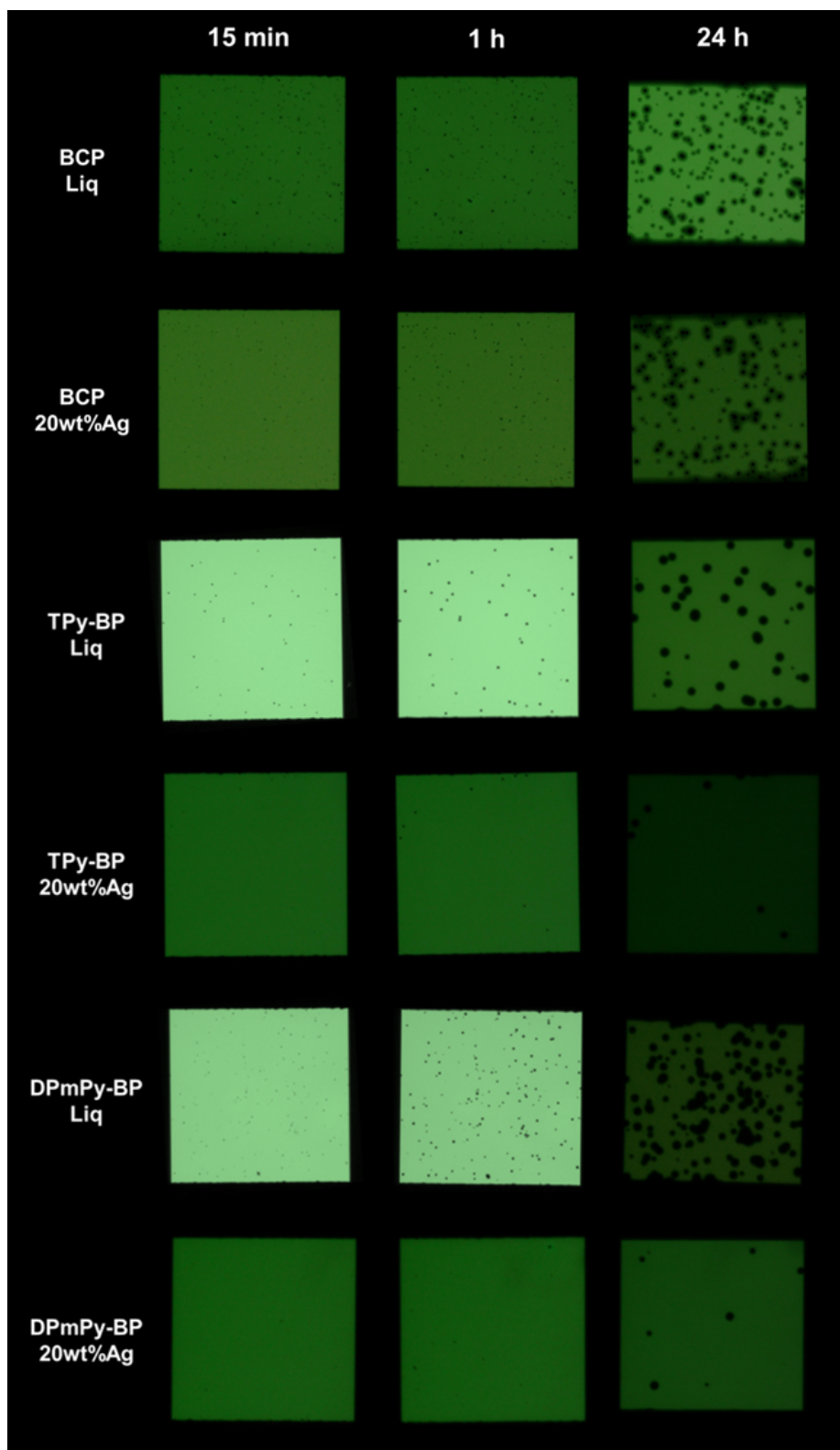


Figure S29. Images of light-emitting areas of devices without encapsulation. 7.0 V dc current was applied to the OLEDs only during measurement and the devices were stored under 295 K, 33% humidity.

7. References

- [1] H. Ishii, D. Tsunami, T. Suenaga, N. Sato, Y. Kimura, M. Niwano, *J. Surf. Sci. Soc. Jpn.* **2007**, 28, 264.
- [2] *CrysAlisPro CCD, CrysAlisPro RED and ABSPACK in CrysAlisPro RED*. Oxford Diffraction Ltd, Abingdon, England (**2006**).
- [3] G. M. Sheldrick, SHELXT – Integrated Space-Group and Crystal-Structure Determination. *Acta Crystallogr., Sect. A: Found. Adv.* **2015**, 71, 3.
- [4] C. Kabuto, S. Akine, T. Nemoto, E. Kwon, Release of Software (Yadokari-XG 2009) for Crystal Structure Analyses. *Nihon Kessho Gakkaishi* **2010**, 51, 218.
- [5] Y. Liu, J. Guo, R. Liu, Q. Wang, X. Jin, L. Ma, W. Lv, S. Liu, S. Yuan, H. Zhu, *J. Lumin.* **2015**, 157, 249-256.